Environ Geol (2009) 58:761–777
DOI 10.1007/s00254-008-1550-3

ORIGINAL ARTICLE

Environmental assessment of the arsenic-rich, Rodalquilar gold–(copper–lead–zinc) mining district, SE Spain: data from soils and vegetation

Roberto Oyarzun · Paloma Cubas · Pablo Higueras · Javier Lillo · Willians Llanos

Received: 26 April 2008 / Accepted: 10 September 2008 / Published online: 30 September 2008

Abstract The Rodalquilar mineral deposits (SE Spain) were formed in Miocene time in relation to caldera volcanic episodes and dome emplacement phenomena. Two types of ore deposits are recognized: (1) the El Cinto epithermal, Au–As high sulphidation vein and breccia type; and (2) peripheral low sulphidation epithermal Pb–Zn–Cu–(Au) veins. The first metallurgical plants for gold extraction were set up in the 1920s and used amalgamation. Cyanide leaching began in the 1930s and the operations lasted until the mid 1960s. The latter left a huge pile of $\sim$900,000–1,250,000 m^3 of abandoned As-rich tailings adjacent to the town of Rodalquilar. A frustrated initiative to reactivate the El Cinto mines took place in the late 1980s and left a heap leaching pile of $\sim$120,000 m^3. Adverse mineralogical and structural conditions favoured metal and metalloid dispersion from the ore bodies into soils and sediments, whereas mining and metallurgical operations considerably aggravated contamination. We present geochemical data for soils, tailings and wild plant species. Compared to world and local baselines, both the tailings and soils of Rodalquilar are highly enriched in As (mean concentrations of 950 and 180 $\mu g\ g^{-1}$, respectively). Regarding plants, only the concentrations of As, Bi and Sb in *Asparagus horridus*, *Launaea arborescens*, *Salsola genistoides*, and *Stipa tenacissima* are above the local baselines. Bioaccumulation factors in these species are generally lower in the tailings, which may be related to an exclusion strategy for metal tolerance. The statistical analysis of geochemical data from soils and plants allows recognition of two well-differentiated clusters of elements (As–Bi–Sb–Se–Sn–Te and Cd–Cu–Hg–Pb–Zn), which ultimately reflect the strong chemical influence of both El Cinto and peripheral deposits mineral assemblages.

Keywords Rodalquilar · SE Spain · Soils · Plants · Arsenic · Contamination

R. Oyarzun (✉) · W. Llanos
Departamento de Cristalografía y Mineralogía,
Facultad de Ciencias Geológicas,
Universidad Complutense, 28040 Madrid, Spain
e-mail: oyarzun@geo.ucm.es

P. Cubas
Departamento de Biología Vegetal II,
Facultad de Farmacia, Universidad Complutense,
28040 Madrid, Spain

P. Higueras
Departamento de Ingeniería Geológica y Minera,
Escuela Universitaria Politécnica de Almadén,
Universidad de Castilla-La Mancha,
Plaza M. Meca 1, 13400 Almadén, Spain

J. Lillo
Escuela Superior de Ciencias Experimentales y
Tecnología, Universidad Rey Juan Carlos,
Tulipán s/n, 28933 Móstoles, Madrid, Spain

Introduction

The Rodalquilar gold mining district (all mines and metallurgical plants presently decommissioned) is located in the Almería province (SE Spain), within the Cabo de Gata—Níjar Natural Park (Fig. 1). The park encompasses about 457 km^2 of protected land and sea (Fig. 1) and is located in the most arid part of Europe, where volcanic outcrops characterize a landscape, in which Mediterranean plant communities grow. The region has a high floristic diversity and is considered a priority for conservation in Europe. The climate is semi-arid Mediterranean, with low

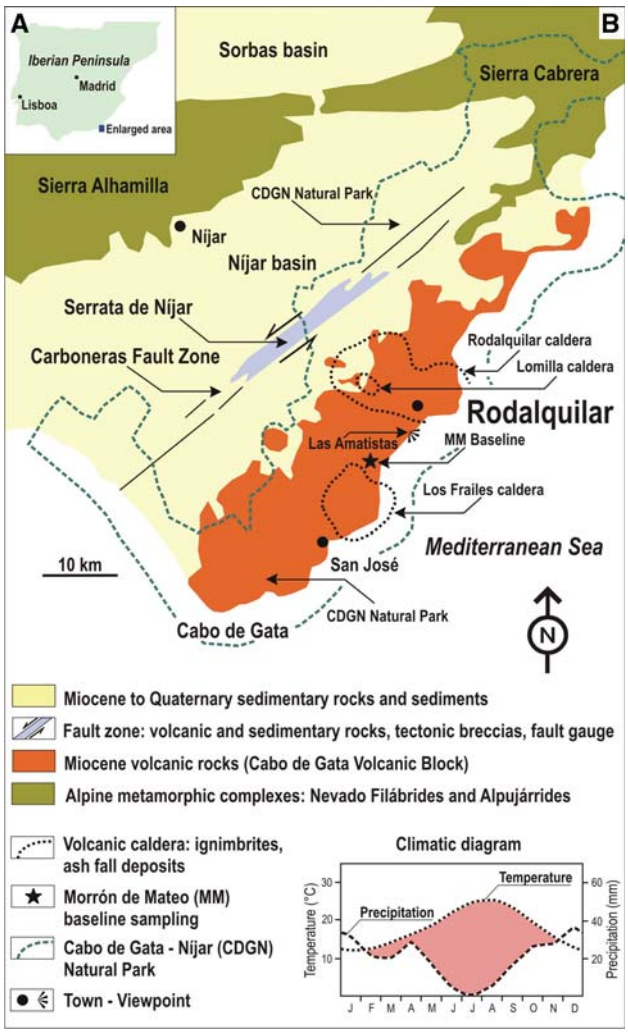

Fig. 1 Geology of the Cabo de Gata region and climatic diagram

annual rainfall and a hot and dry summer (Fig. 1). Mean annual temperature and precipitation are 18°C and 200 mm, respectively. From a physiographic point of view, the Rodalquilar district is located within a hilly environment with maxima altitudes of 360–380 and 100–200 m deep relatively narrow valleys (Fig. 2a). The latter coalesce into larger "ramblas" (a Spanish term for dry ravine), which are dry most of the year, but may behave as high-flow torrents during short periods of strong rains. The Rodalquilar district has received the attention of many workers, who have studied the zone from the metallogenic (Rytuba et al. 1990; Arribas et al. 1995; among others), environmental (Wray 1998; Ferrier 1999; Moreno et al. 2007), historical (Hernández Ortiz 2004; Hernández 2005) and educational (Oyarzun et al. 2007a) points of view. Previous environmental studies focused on: (1) the tailings and dispersion of trace metals in sediments (Wray 1998); (2) the characterization and dispersion of iron species from the tailings (Ferrier 1999); and (3) the mineralogical and chemical characterization of the aerial particulate (PM_{10}) derived from the tailings (Moreno et al. 2007). However, some key aspects of the environmental disturbances derived from past mining activities were not addressed in the previous works. In this regard, we may highlight the following: (1) the study of the cyanide heap leaching operation that started in 1989 and left abandoned tailings on the western sector of the district; (2) a systematic geochemical survey of soils; and finally yet importantly, (3) a study on metal accumulation by plants. We took soil and mineral waste samples from the whole district and centred our vegetation sampling on perennials plants (*Launaea arborescens*, *Lygeum spartum*, *Salsola genistoides*, *Stipa tenacissima*) (Fig. 3a–c) and a wild asparagus (*Asparagus horridus*). These species are well represented in the area and grow on different substrates. Given the natural park status of the area, no plants were uprooted during the survey. Besides, none of the chosen plant species is included in any endangered species checklist.

Geology, mineral deposits and mining-metallurgical operations

Regional geology

Southeast Spain hosts the 160 km long Almería–Cartagena Volcanic Belt (ACVB) (Oyarzun et al. 1995). This coastal Miocene belt comprises a variety of volcanic series including calc-alkaline, high-K calc-alkaline, and shoshonitic rocks. The Almería sector of the belt is also characterized by the presence of two of the most important Alpine metamorphic complexes of southern Spain: Alpujarride and Nevado Filábrides (Fig. 1). These units were intensively folded during late Oligocene–Early Miocene, and later underwent extensional collapse through major detachment systems in Middle-Late Miocene time (e.g., Doblas and Oyarzun 1989; Platt and Vissers 1989). The latter episode was accompanied by calc-alkaline volcanism (andesites, dacites, rhyolites) and sedimentation within evaporitic sedimentary basins (e.g., Sorbas and Níjar) (Fig. 1). Subsequent large, ENE–WSW sinistral wrench faulting gave rise to the Carboneras Fault Zone (Huibregtse et al. 1998; Keller et al. 1997). The Cabo de Gata volcanic block (Fig. 1) comprises a wide variety of volcanic rocks of generally decreasing age from WSW to ENE. These rocks include the ~15 Ma old Cabo de Gata andesites, the 14–12 Ma old dacites to andesites of the Los Frailes (San José) caldera, and the 11–8 Ma old ignimbrites, felsic domes and pyroxene andesites of Rodalquilar (Oyarzun et al. 1995; Arribas et al. 1995).

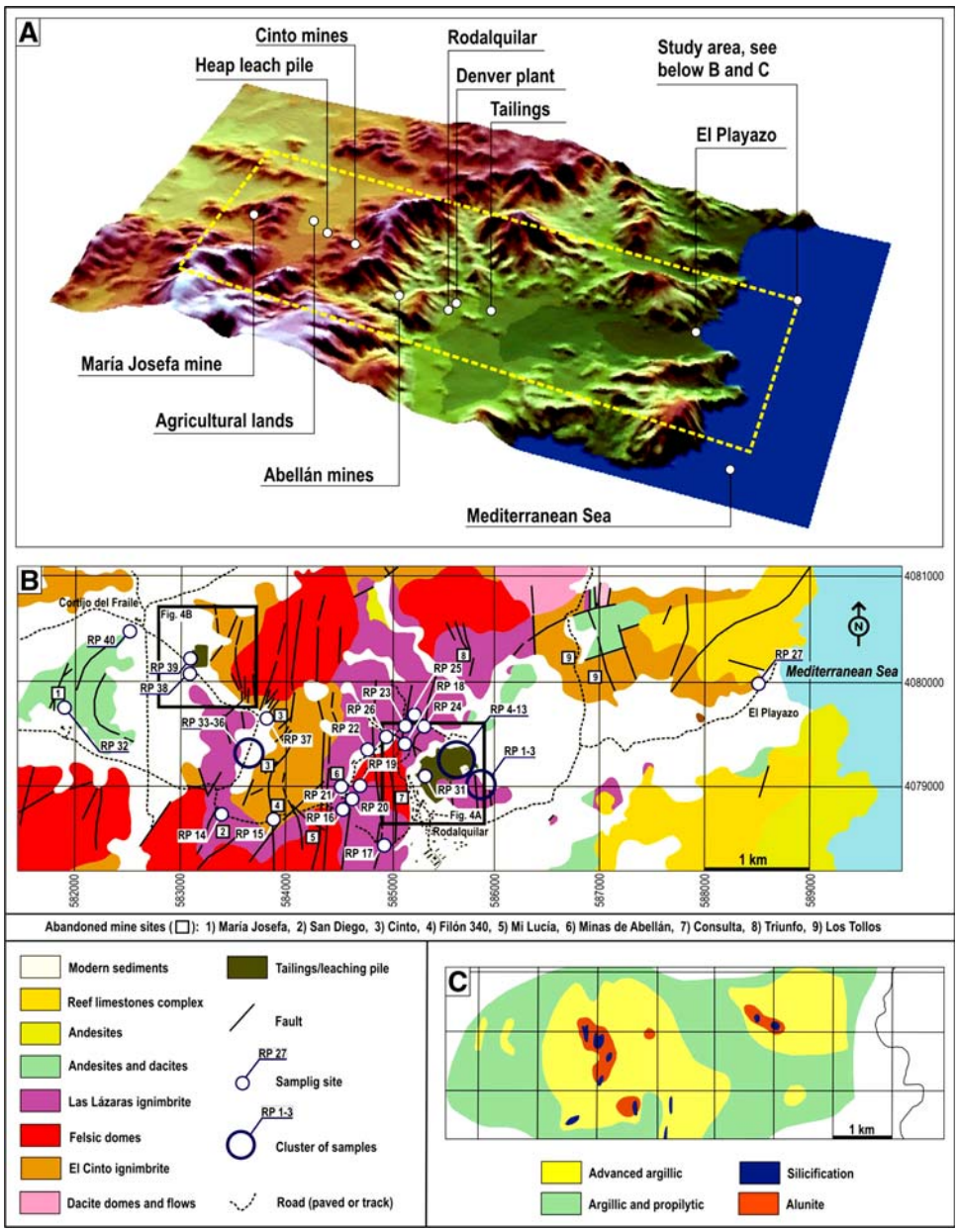

Fig. 2 The Rodalquilar district. **a** digital elevation model for Rodalquilar displaying major features of environmental interest (mines, tailings, metallurgical plants, etc.); **b** geology of the Rodalquilar district and abandoned mines (simplified after Arribas 1993), location of samples and tailings deposits (this work); **c** hydrothermal alteration in the Rodalquilar district (same UTM coordinate system as in **b**) (after Arribas et al. 1995). See details from *inlets* (*thick black line squares*) in Fig. 4a, b, respectively

The Rodalquilar district

The geologic setting of Rodalquilar district (Rytuba et al. 1990; Arribas 1993; Arribas et al. 1995) includes Upper Miocene felsic domes, ignimbrites, ash fall deposits, massive volcanic rocks, and a limestone complex of Messinian age (Fig. 2b). Magmatic activity began at about 11 Ma ago with the emplacement of dacite domes and flows, an episode that was followed shortly by explosive volcanic activity that led to formation of the large, E–W elongated El Cinto caldera, and the small, WNW–ESE oriented Lomilla caldera (Arribas et al. 1995) (Fig. 1). The El Cinto episode is dated at 10.8 Ma, and gave rise to the, so-called, El Cinto ignimbrite. Immediately after the area was pervaded by the emplacement of ring dome complexes of rhyolitic composition. The pyroclastic activity ended with formation of the La Lomilla caldera and the emission of the Las Lázaras ignimbrite (Arribas 1993; Arribas et al. 1995). Two more volcanic episodes are recorded in the area, one at 9 Ma with andesites and dacites, and a final one at 8 Ma with pyroxene andesites (Arribas 1993). From a metallogenic point of view, the ring dome complexes and the El Cinto and Las Lázaras ignimbrites are the most important units as they host a variety of mineral deposits of economic importance. Mineral deposits include those of the epithermal Au–As high sulphidation vein and breccia type (El Cinto deposits), and low sulphidation (peripheral) epithermal Pb–Zn–Cu–(Au) veins (e.g., María Josefa) (Fig. 2b). Mineralizing

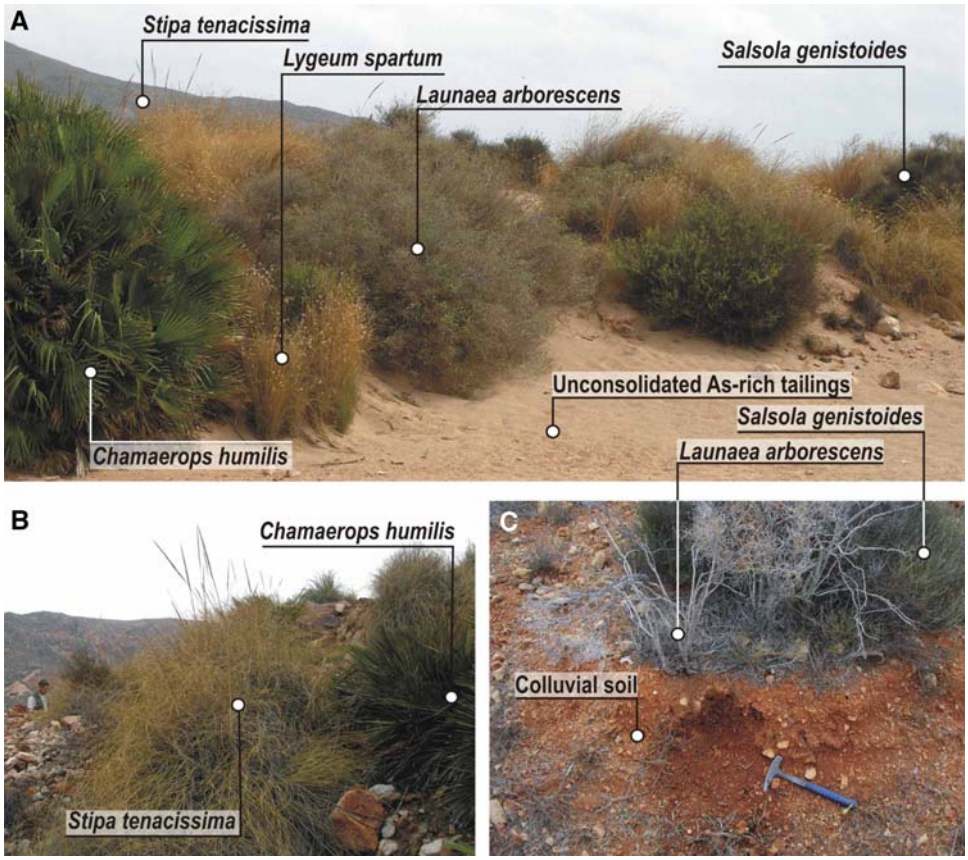

Fig. 3 The studied wild plant species in different locations: **a** strong and diverse plant community growing on the lower tailings sandy-silty technosols, near to sample RP-8; **b** *Stipa tenacissima* and *Chamaerops humilis* (not studied in this work) growing alongside the road from Rodalquilar to the El Cinto mines, near to sample RP-18; **c** *Launaea arborescens* and *Salsola genistoides* growing on a typical Rodalquilar inceptisol developed on colluvial materials (*image* colluvial soil), near to sample RP-23. See also Fig. 2b for sample locations. The photographs were taken between the 11th and 13th of September 2007

processes have been dated at about 10.4 Ma, and were accompanied by widespread hydrothermal alteration including zones of strong silicification, alunitization, advanced argillic and argillic-propylitic (Arribas et al. 1995) (Fig. 2c). Massive oxidation of primary sulphides (mostly pyrite) and subsequent formation of acid solutions at about 3 Ma led to mineral overprinting by clay and alunite formation over the previous hydrothermal assemblages. The primary ore mineralogy of the El Cinto deposits is characterized by the presence of native gold, pyrite (FeS_2), enargite (Cu_3AsS_4), tennantite ($Cu_{12}As_4S_{13}$), tetrahedrite ($Cu_{12}Sb_4S_{13}$), cinnabar (HgS), bismuthinite (Bi_2S_3), cassiterite (SnO_2), galena (PbS) and sphalerite (ZnS). On the other hand, the primary ore mineralogy of the peripheral low sulphidation deposits consists of native gold, sphalerite (ZnS), galena (PbS), and chalcopyrite ($CuFeS_2$) (Arribas et al. 1995). Apart from the ore deposit types described above, we must highlight the alunite veins (the so-called *tollos*) that, in older times, were economically exploited in the Rodalquilar district and elsewhere in SE Spain.

Mining and metallurgical operations

Given that heavy metal contamination in the Rodalquilar district is strongly related to mining (abandoned cavities, mineral dumps) and metallurgical operations (abandoned plants and tailings) (e.g., Wray 1998; Ferrier 1999; Moreno et al. 2007), we briefly review here the history of both industrial activities. Mining in the Rodalquilar district (Hernández 2005) initiated around 1825 for Pb, Zn, and Cu, and it was not until 1864 that the miners realized that the ore contained some gold as well. Mining operations belonging to this period are those of Consulta, María Josefa, San Diego and Triunfo (Fig. 2b). These were small-scale operations and the ore was sent to Murcia for the melting and production of Au-rich Pb. In 1925, a metallurgical operation for gold amalgamation with mercury at the María Josefa mine was set up (Fig. 2b), however, a year later technical problems led to the closure of the operation. Another failed gold amalgamation operation was carried out between 1929 and 1930 at the Minas de Abellán (Fig. 2b) (Hernández Ortiz 2004). Modern mining in Rodalquilar initiates in 1931 with the set up of the first cyanide leaching metallurgical operation (the Dorr plant) near the town of Rodalquilar. Similar to modern heap leaching for gold extraction, the process used cyanide to complex gold. The plant received ore from the Consulta, Triunfo and Mi Lucía mines (Hernández 2005) (Fig. 2b). In 1956, the mining company ADARO (a state owned enterprise) inaugurated a new cyanide operation at the new

Denver plant, which at the time was the largest leaching plant in Europe (Fig. 4a). This operation lasted until 1966 and treated ore from the open pit mines of El Cinto (Fig. 4c) (Hernández 2005). Between 1943 and 1966, ADARO extracted some 1.6 Mt (10^6 metric tons) of ore grading 3.5 g t^{-1} Au ($\sim$180,000 oz Au) (Ormonde Mining 2002). Most, if not all, of the tailings around the town of Rodalquilar can be related to this mining period (Figs. 2b, 4a). Based on production data for the period 1943–1966 (Ormonde Mining 2002; Hernández Ortiz 2004), the volume of the tailings may be in the range of 900,000–1,250,000 m^3. These deposits are divided in two sectors: (1) the lower (older) tailings, which are partially contained by a severely deteriorated dam (Fig. 4d). These deposits have been long colonized by a strong community of *S. tenacissima*, *L. spartum*, *L. arborescens* and *S. genistoides*, and other wild plants including the dwarf, endemic Spanish palm "palmito" (*Chamaerops humilis*) (not studied in this work) (Fig. 3a). (2) The upper (younger) tailings, which are contained by a large earth dam. There is a network of stone low walls forming stabilization plots on the top of the upper tailings (Fig. 4a) that was presumably built to pond rainfall and minimize erosion (Wray 1998). The tailings have been partially covered with $\sim$10 cm of gravels (Fig. 4e), and for a number of years, there has been an attempt to use the stabilization plots to grow wild native

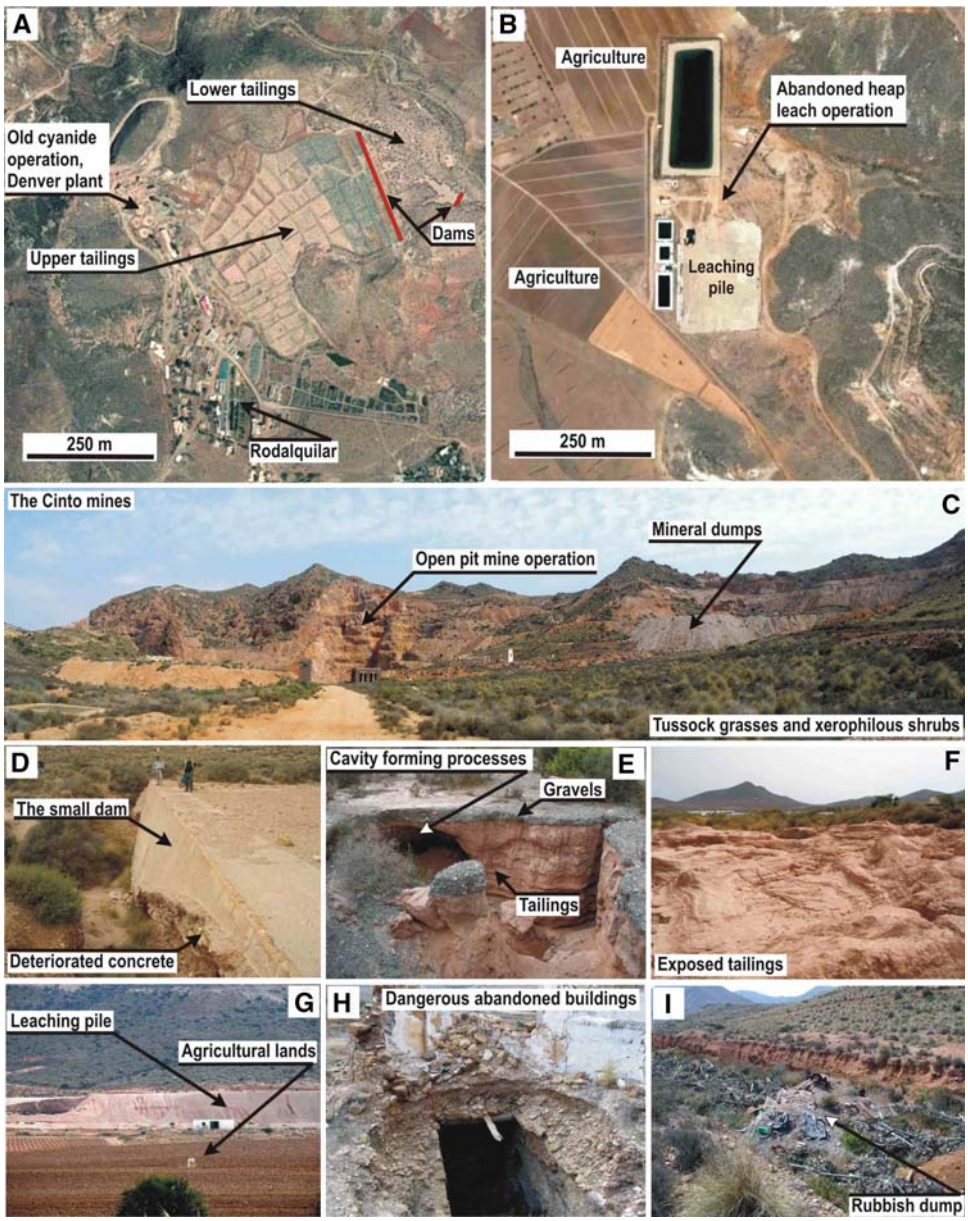

Fig. 4 The Rodalquilar district: environmental hazards. **a** Tailings, dams, and the abandoned Denver leaching plant (see *right inlet* in Fig. 2b); **b** the abandoned heap leaching operation and agricultural lands (see *left inlet* in Fig. 2b); **c** the El Cinto open pit mines; **d** the lower tailings dam showing severe deterioration; **e** cavity forming processes in the upper tailings; **f** uncovered upper tailings deposits; **g** the abandoned heap leaching pile and presently worked agricultural lands (see also **b**); **h** safety risks posed by abandoned buildings (María Josefa mine); **i** old roads converted into rubbish dumps (southern access to the El Cinto mines). The photographs were taken between the 11th and 13th of September 2007

plant communities and introduced species. A couple of plots have been left uncovered (Fig. 4f). Drip irrigation is used in this sector, which minimizes the use of water by allowing it to drip slowly to the roots through a network of valves, pipes, tubing, and emitters. In this regard, we noted severe cavity forming phenomena in the tailings, which seem to be caused by water losses from the pipes (Fig. 4e). Besides, it comes as an irony, those wild plant communities (Fig. 3a) grow stronger in the lower tailings (where no irrigation system was ever devised) than in the upper ones.

Despite the Rodalquilar district is well inside the Cabo de Gata—Níjar natural Park (declared as such in 1987), a new mining and metallurgical operation in the El Cinto sector began in 1989. This time the company was foreign (Cluff Resources—Antofagasta Holdings JV) and the chosen metallurgical procedure was heap leaching (Fig. 2b, 4b). The intention was to mine some 750,000 metric tons of ore at 2.3 g t^{-1} Au, although by 1990 the operation was abandoned (Hernández 2005). As the result of this failed operation, some 120,000 m^3 of tailings (abandoned pile) still remain there, near to the Cortijo del Fraile, in close proximity to agricultural lands (Fig. 4b, g).

Materials and methods

The geochemical survey was carried out in September 2007, and 35 samples of soils and 91 samples of plants were taken. Based on the mineralogy of the Rodalquilar deposits and that of the mine wastes, we chose, for this study, the following chemical elements: As, Cu, Cd, Hg, Pb, Sb, Se, Sn, Te, and Zn. Given the amalgamation practices carried out in the early twentieth century, we additionally measured Hg (gas) in the district.

Soils

Special consideration was given to the criteria used for selection of sampling sites of soils and plants. Given that the topsoil is the most important part of the soil profile for degradation control (Spaargaren and Nachtergaele 1998), we took samples from the first 30 cm, because it is within this region where *Lygeum spartum*, *Salsola genistoides*, and *Stipa tenacissima* have the highest root density (90–100%) (De Baets et al. 2007). The soils of Rodalquilar can be classified as inceptisols and anthrosols. The Rodalquilar inceptisols exhibit minimal horizon development and formed in colluvial deposits that typically occur on the sloping landscapes of the district (Fig. 3c). They consist of mixed deposits of rock fragments (usually ignimbrite clasts) and brown to reddish-brown sandy to silty materials. The anthrosols are soils that underwent profound modification by human activities (e.g., mining, road construction). The latter also have properties of the technosols (Rossiter 2005), that is, we are dealing with recent (less than a hundred years old) deposits of artificial origin such as the tailings that nevertheless have already developed important wild plant communities (Fig. 3a). The soil samples (~2 kg) were stored in plastic bags, sieved at the Almadén School of Mines (ASM; Universidad de Castilla La Mancha), and part of the sample sent to Activation Laboratories Ltd. (Actlabs; Canada) to be analyzed by ICP/MS (Inductively Coupled Plasma—Mass Spectrometry). Quality control at the Actlabs laboratory is done by analyzing duplicate samples and blanks to check precision, whereas accuracy is obtained by using certified standards (GXR series). Detection limits for the analyzed elements are (data in μg g^{-1}): As (0.1), Bi (0.02), Cd (0.1), Cu (0.2), Pb (0.5), Sb (0.1), Se (0.1), Sn (1), Te (0.1), Zn (0.2). An aliquot of each soil sample was kept at the ASM laboratory for the analysis of: (1) organic carbon and determination of pH following the International Soil Reference and Information Centre (ISRIC) standard procedures (Van Reeuwijk 2002); and (2) to analyze Hg by pyrolysis (see below for procedures). The mineralogy and mineral chemistry of soils was studied by XRD (instrument: Philips, model PW3040/00 X'Pert MPD/MRD) and SEM-EDX (instrument: Philips XL30; 25 kV) at the CAT facilities of Universidad Rey Juan Carlos (Madrid).

Plants

We focused our vegetation sampling on perennials plants well represented in the area on different substrates, and selected two long-lived tussock grass species (*L. spartum* and *S. tenacissima*), and two xerophilous, perennial shrubs (*L. arborescens* and *S. genistoides*) (Fig. 3a). We added to this list, a wild asparagus "espárrago triguero" (*Asparagus horridus*). *Stipa tenacissima* ("esparto") is a robust caespitose perennial grass (Poaceae) with stems of 60–150 cm. *Lygeum spartum* ("albardin") is also a perennial tussock grass, similar to esparto but smaller in size, although the ecology of the two species is similar. *Launaea arborescens* (Asteraceae) is a xerophilous perennial shrub reaching a height of 50–150 cm (Sagredo 1987). *Salsola genistoides* ("escobilla") (Chenopodiaceae) is a perennial shrub reaching a height of up to 2 m, with stems having numerous longitudinal ridges and small fugacious filiform leaves. *Asparagus horridus* (Asparagaceae) is characterized by a woody stem up to 60 cm long, branches with numerous ridges, and strongly spiny cladodes (modified stems). The collected plant specimens were prepared at the Plant Biology II Department (Universidad Complutense) in Madrid, and voucher specimens are kept presently at the

MAF Herbarium (MAF167306–MAF167401). Given that the plant material was collected after the summer, the aerial parts mostly consisted of dry matter as typically expected in steppe vegetation. We discarded flowers because they were either too small or absent in most of the plants. Based on plant species morphology (habit), we chose stems and branches in *A. horridus*, *L. arborescens*, and *S. genistoides*), and leaves in *L. spartum* and *S. tenacissima*. These parts were thoroughly cleaned with distilled water, air-dried (to avoid heavy losses of Hg), and finally powdered with an electric crusher to reduce size. The samples were sent to Actlabs and analyzed by HR (High Resolution)-ICP/MS. Quality control at the laboratory is done by analyzing duplicate samples and blanks to check precision, whereas accuracy is obtained by using certified standards (NIST SRM 1575a). Detection limits for the analyzed elements are (data in ng g^{-1} except Se and Zn in μg g^{-1}): As (5), Bi (1), Cd (0.1), Cu (20), Hg (5), Pb (10), Sb (0.2), Se (0.2), Sn (40), Te (1), Zn (0.2).

Hg in atmosphere and soils

The analytical procedure is based on Zeeman atomic absorption spectrometry with high frequency modulation of light polarization (ZAAS-HFM) (Sholupov and Ganeyev 1995). The instrument (LUMEX RA-915+) allows determination of Hg in air directly with an ultra low detection limit in real time. This detection limit is governed by shot noise and equals 2 ng m^{-3} (average measuring time: 5 s) and 0.3 ng m^{-3} (average measuring time: 30 s) for mercury determination in air. The dynamic range of the instrument covers 4 orders of magnitude (2–30,000 ng m^{-3}). On the other hand, the RP-91C (pyrolysis) attachment provides the capacity to measure Hg in solid samples. This attachment was used for the analyses of soils at the laboratories of the ASM. As a first step, the sample is vaporized and the Hg compounds partly decomposed. This is followed by heating to 800°C, at which point the Hg compounds become fully decomposed, whereas organic compounds and carbon particles are catalytically transformed to carbon dioxide and water. Quality control at the ASM laboratory is done by analyzing duplicate samples to check precision, whereas accuracy is obtained by using certified standards (NIST SRM 2710 Montana Soil). Detection limit for total Hg is 0.5 μg kg^{-1}.

Results and discussion

General

Trace element concentrations in the 33 samples of soils from the district are shown in Table 1, whereas basic statistical data (mean, standard deviation) for trace element concentrations in the five plant species (91 samples) are shown in Table 2. As shown by Wray (1998) and Moreno et al. (2007), the Rodalquilar tailings (here regarded as technosols) (Figs. 2a,b, 4a) appear as one the most important environmental hazard in the district. For example, these authors found As concentrations in the tailings in the range of 421–1337 μg g^{-1}. They also indicate that: (1) the metals and metalloids from the tailing are found at elevated concentrations in stream sediments down to El Playazo (Wray 1998) (Fig. 2a); and (2) the tailings also provide a point source for contaminated wind blown dust (Moreno et al. 2007). Our district-wide geochemical survey of both soils (Table 1) and plants (Table 2) confirm these results and expand the environmental concerns to other areas of the district. Two of these sectors include the María Josefa mine, and the heap leaching pile of El Cinto, which are either close or adjacent to agricultural lands (Figs. 2a,b, 3a,b, 4a–g). This is not surprising for a long-lived mining-metallurgical site such as Rodalquilar, because as indicated by Ownby et al. (2005), many environmental problems worldwide can be attributed to past metal mining and smelting activities. However, the important questions to be addressed here is why and how this happened in Rodalquilar.

Factors controlling metal dispersion-fixation

As observed elsewhere in similar settings (Oyarzun et al. 2004, 2007b), key factors controlling the environmental behavior of epithermal mineral deposits include ore and gangue mineralogy, host rock lithology, fracturing, wall-rock alteration and climate, which influence the chemical response of mineral deposits. The El Cinto type Rodalquilar ore deposit has a strong and extensive advanced argillic alteration zone (Fig. 2c). This has profound implications regarding metal dispersion, because this type of alteration greatly decreases the acid buffering capacity of the host rocks (Plumlee 1999; Plumlee et al. 1999; Oyarzun et al. 2007b). The chemistry of these processes can be summarized in the following way. Enhanced hydrolysis during hydrothermal activity leads to the destruction of feldspars, through subsequent formation of sericite (1), kaolinite (2), and even alunite (3) if H_2SO_4 is present in the system (Montoya and Hemley 1975), which is common in high sulphidation (acid sulphate) systems (Heald et al. 1987):

$$3KAlSi_3O_8 + 2H^+ \rightarrow KAl_3Si_3O_{10}(OH)_2 + 6SiO_2 + 2K^+ \quad (1)$$

$$2KAl_3Si_3O_{10}(OH)_2 + 2H^+ + 3H_2O \rightarrow 3Al_2Si_2O_5(OH)_4 + 2K^+ \quad (2)$$

Table 1 Trace element concentration in soils

Element (μg g^{-1})[a]	As	Bi	Cd	Cu	Hg (ng g^{-1})	Pb	Sb	Se	Sn	Zn
RP-1	38.1	1.4	0.2	25.8	125.0	222.0	0.6	3.0	5.0	33.8
RP-2	70.4	0.9	0.2	31.1	165.0	141.0	4.7	3.1	6.0	81.1
RP-3	57.3	0.4	0.2	39.9	244.0	87.6	2.0	4.4	4.0	62.5
RP-4	784.0	10.1	0.7	168.0	599.0	798.0	40.5	27.5	36.0	305.0
RP-5	110.0	1.4	0.6	102.0	114.0	266.0	8.1	4.6	5.0	266.0
RP-6	697.0	10.2	0.2	90.9	274.0	467.0	36.3	24.7	38.0	107.0
RP-7	604.0	11.9	0.1	63.6	142.0	135.0	32.2	22.7	33.0	75.0
RP-8	992.0	17.5	0.2	137.0	178.0	173.0	31.9	32.6	37.0	120.0
RP-9	914.0	8.9	0.1	50.6	159.0	92.7	28.1	35.6	47.0	83.0
RP-10	1,140.0	21.3	0.4	169.0	702.0	475.0	62.6	34.6	76.0	269.0
RP-11	1,240.0	9.9	0.1	39.8	240.0	80.2	37.9	37.1	108.0	160.0
RP-12	1,260.0	73.5	0.1	90.4	248.0	144.0	62.0	44.5	60.0	111.0
RP-13	1,340.0	19.7	0.2	135.0	218.0	381.0	48.0	34.1	67.0	257.0
RP-14	27.4	2.0	0.1	17.6	266.0	28.2	3.9	3.2	8.0	1.3
RP-15	110.0	1.0	0.2	69.9	474.0	252.0	2.8	4.1	8.0	62.7
RP-18	198.0	4.1	0.1	25.8	2,360.0	200.0	6.6	14.7	11.0	42.4
RP-21	89.7	1.0	0.2	90.3	230.0	153.0	5.6	8.3	6.0	77.2
RP-22	169.0	7.4	0.1	60.0	2,570.0	115.0	11.3	16.1	15.0	27.0
RP-23	61.3	1.0	0.8	75.8	65.0	270.0	2.5	1.5	4.0	401.0
RP-24	218.0	19.9	0.1	178.0	404.0	250.0	27.8	13.0	16.0	30.2
RP-25	126.0	2.4	0.8	45.8	61.0	378.0	6.4	3.9	11.0	136.0
RP-26	125.0	0.8	0.2	20.6	824.0	193.0	3.8	4.1	5.0	60.5
RP-27	35.1	0.0	0.1	11.2	192.0	56.3	7.3	8.9	3.0	9.5
RP-28	45.8	0.1	0.2	14.9	77.0	40.1	4.6	2.2	2.0	56.2
RP-31	1,510.0	21.4	0.5	155.0	1,410.0	380.0	51.3	49.8	95.0	288.0
RP-32	1,280.0	8.0	5.7	701.0	704.0	5,000.0	53.2	5.8	34.0	3,430.0
RP-33	301.0	4.1	0.2	45.9	249.0	242.0	13.0	16.8	26.0	71.9
RP-34	195.0	4.9	0.1	57.5	254.0	225.0	18.5	8.4	15.0	39.7
RP-35	69.9	1.8	0.1	120.0	566.0	314.0	8.3	2.0	6.0	35.8
RP-37	292.0	2.8	0.1	55.7	136.0	110.0	22.0	14.2	28.0	49.5
RP-38	159.0	1.6	0.2	44.6	44.0	166.0	10.7	4.7	9.0	122.0
RP-39	859.0	5.8	0.1	68.8	84.0	64.5	19.8	50.3	58.0	12.1
RP-40	104.0	0.6	0.5	51.5	77.0	181.0	1.2	2.6	5.0	246.0
RP-29[b]	21.0	<0.1	0.1	13.8	122.0	31.0	0.2	1.1	0.5	54.1
RP-30[b]	5.3	<0.1	0.1	14.4	50.0	35.0	0.5	1.0	4.0	53.9

See Fig. 2b for location

[a] Unless indicated

[b] Morrón de Mateo (MM) baselines; see Fig. 1 for location

$$KAl_3Si_3O_{10}(OH)_2 + 4H^+ + 2(SO_4)^{2-} \rightarrow KAl_3(SO_4)_2(OH)_6 + 3SiO_2 \quad (3)$$

This is particularly relevant to the case of high sulphidation epithermal deposits (such as El Cinto), which are rich in pyrite and other sulphides (Heald et al. 1987). Thus, when oxidation of pyrite begins in the weathering environment, no minerals (such as feldspars) are left to react with the acid and ferric sulphate generated during the oxidation of pyrite (4–6), which greatly increases metal mobility from other sulphides, among them, enargite (7):

$$FeS_2 + 3.5O_2 + H_2O = Fe^{2+} + 2SO_4^{2-} + 2H^+ \quad (4)$$

$$Fe^{2+} + 0.25O_2 + H^+ = Fe^{3+} + 0.5H_2O \quad (5)$$

$$4FeS_2 + 10H_2O + 15O_2 \rightarrow 4FeO(OH) + 16H^+ + 8SO_4^{-2} \quad (6)$$

$$Cu_3AsS_4 + 5.5Fe_2(SO_4)_3 + 4H_2O \rightarrow 3CuSO_4 + 11FeSO_4 + 4S + H_3AsO_4 + 2.5H_2SO_4 \quad (7)$$

Contrary to what might be expected in soils from arid regions, the XRD studies indicated the widespread

Table 2 Trace element concentration in plant species

Element (ng g^{-1})[a]	As	Bi	Cd	Cu	Hg	Pb	Sb	Se (μg g^{-1})	Sn	Te	Zn (μg g^{-1})
All plant species											
All soils											
Mean ($n = 83$)	1,129.1	30.6	272.7	7,295.7	43.1	1,568.2	169.0	1.2	94.9	16.6	36.3
SD	1,400.9	69.7	691.4	8,416.3	51.7	1,740.0	257.6	2.2	92.2	21.5	32.9
Tailings											
Mean ($n = 31$)	2,380.1	67.0	150.7	7,458.4	28.2	1,421.6	332.9	2.0	149.4	32.9	38.2
SD	1,610.6	104.9	192.2	7,353.9	11.4	1,048.8	345.8	2.4	119.6	27.7	26.2
Baseline Morrón de Mateo (MM)											
MM − 1 (RP29) ($n = 4$)	235.3	4.3	678.6	5,475.0	31.8	887.5	38.8	0.5	47.5	3.0	37.0
MM-2 (RP30) ($n = 4$)	244.5	6.0	133.9	4,722.5	39.5	1,812.5	52.4	0.3	60.0	2.5	18.0
Asparagus horridus											
All soils											
Mean ($n = 14$)	555.7	17.9	27.1	2,280.7	14.9	827.1	123.2	0.6	75.7	8.9	43.6
SD	534.8	22.4	18.7	743.7	8.1	716.6	145.2	0.3	61.1	10.8	45.3
Tailings											
Mean ($n = 5$)	1,120.0	39.6	20.5	2,600.0	12.0	768.0	247.1	0.8	122.0	18.8	29.9
SD	477.3	26.0	11.6	634.0	3.1	220.3	162.5	0.4	81.1	13.1	13.5
Baseline Morrón de Mateo (MM)											
MM-1 (RP29)	166.0	3.0	18.1	1,520.0	13.0	670.0	33.7	0.6	50.0	5.0	53.6
MM-2 (RP30)	110.0	4.0	35.0	2,380.0	15.0	620.0	34.9	0.3	50.0	0.5	32.9
Launaea arborescens											
All soils											
Mean ($n = 25$)	1,066.8	16.9	618.3	13,288.4	69.8	1,776.4	116.7	2.1	76.8	11.7	42.8
SD	1,261.6	12.5	1,179.1	11,691.7	82.4	2,421.2	131.9	2.9	61.2	8.2	38.7
Tailings											
Mean ($n = 10$)	2,038.0	24.9	245.8	13,154.0	30.9	669.0	134.9	2.4	67.0	15.9	38.2
SD	1,523.0	13.1	256.8	9,355.7	7.8	337.6	80.7	1.9	49.2	9.7	17.3
Baseline Morrón de Mateo (MM)											
MM-1 (RP29)	502.0	6.0	2,380.0	16,100.0	61.0	1,350.0	65.9	1.1	80.0	0.5	79.8
MM-2 (RP30)	507.0	10.0	145.0	10,800.0	58.0	2,960.0	77.2	0.5	90.0	4.0	21.5
Lygeum spartum[b]											
All soils											
Mean ($n = 14$)	2,365.2	94.4	86.5	2,192.1	36.7	1,819.3	388.6	1.8	177.1	40.1	24.5
SD	2,073.6	152.4	51.5	1,037.0	10.1	925.7	477.8	3.4	130.6	38.3	7.6
Tailings											
Mean ($n = 7$)	4,037.1	175.3	98.3	1,890.0	33.9	2,190.0	710.3	3.4	282.9	71.1	26.0
SD	1,604.5	187.1	60.1	428.0	9.0	902.0	501.5	4.4	95.3	74.2	24.6
Salsola genistoides											
All soils											
Mean ($n = 19$)	851.1	19.3	261.9	9,301.6	41.3	1,786.3	130.2	0.6	74.2	15.5	41.1
SD	1,008.9	26.7	229.3	5,816.9	33.7	1,949.2	190.7	0.5	82.7	16.1	31.2
Tailings											
Mean ($n = 7$)	1,803.4	41.4	190.7	9,564.3	29.1	2,224.3	274.6	1.0	127.1	30.4	63.4
SD	1,118.6	34.6	209.8	4,120.0	13.3	1,305.5	260.5	0.4	113.1	17.5	40.1
Baseline Morrón de Mateo (MM)											
MM-1 (RP29)	158.0	4.0	271.0	3,090.0	31.0	750.0	31.2	0.3	40.0	6.0	7.1
MM-2 (RP30)	128.0	3.0	315.0	3,500.0	56.0	1,190.0	50.9	0.1	40.0	5.0	6.0

Table 2 continued

Element (ng g^{-1})[a]	As	Bi	Cd	Cu	Hg	Pb	Sb	Se (μg g^{-1})	Sn	Te	Zn (μg g^{-1})
Stipa tenacissima											
All soils											
Mean ($n = 11$)	907.6	16.5	55.4	3,089.1	29.2	1,341.8	133.9	0.3	91.8	9.8	18.8
SD	1,291.9	21.9	33.1	1,089.2	13.6	1,011.7	176.3	0.5	99.0	11.2	5.3
Tailings (2 samples)											
RP9	3,670.0	74.0	56.4	4,670.0	40.0	1,640.0	566.0	0.6	370.0	35.0	11.5
RP10	3,250.0	40.0	32.7	1,820.0	23.0	1,000.0	276.0	1.7	110.0	21.0	14.3
Baseline Morrón de Mateo											
MM-1 (RP29)	115.0	4.0	45.1	1,190.0	22.0	780.0	24.2	0.1	20.0	0.5	7.6
MM-2 (RP30)	233.0	7.0	40.4	2,210.0	29.0	2,480.0	46.7	0.1	60.0	0.5	11.5

[a] ng g^{-1} unless indicated

[b] No plants of *Lygeum spartum* were present at Morrón de Mateo (Fig. 1)

presence of kaolinite in most of the studied samples (RP 7, 8, 11, 12, 23, 39). Its origin can be assigned to either the hydrolysis of feldspars during hydrothermal alteration of rocks (2) or to the acidic conditions triggered by the supergene alteration of pyrite. Alunite was also found in the tailings and pile samples (RP 7, 8, 11, 12, 39), which also supports the acidic conditions that were generated during hydrothermal and supergene alteration at El Cinto deposits. On the contrary, the only sample with montmorillonite (RP-32) corresponds to a soil from María Josefa, which is a peripheral mineral deposit, far away from the core of advanced argillic alteration. Although kaolinite has a net zero layer charge, a small negative charge at the broken edges can be responsible for the adsorption of metals. Thus, even if kaolinite is the least reactive clay, its high pH dependency enhances or inhibits the adsorption of metals according to the pH of the soil. On the other hand, montmorillonite has a net negative charge of 0.8 units per unit cell and this has been responsible for giving superior activity to montmorillonite as an adsorbent for heavy metals (Bhattacharyya and Gupta 2008). Compared to kaolinite, montmorillonite has a very large adsorption capacity for heavy metals (e.g., Cd, Cr, Co, Cu, Pb, Ni) with values that can be 2–3 times higher (Bhattacharyya and Gupta 2008). Besides, there is widespread field (this work) and remote sensing (Ferrier 1999) evidence in the Rodalquilar district for strong leaching and oxidation of the mineralized veins to goethite and jarosite. Furthermore, the district has a dense fracturing system that first enhanced hydrothermal circulation, and later facilitated oxidation and leaching. Another key factor controlling metal dispersion in the environment is climate. The semi arid climate of the region may have started as early as ~4500 BP, with a radical transformation of the landscape that reflects in the establishment of the steppe conditions found today (Pantaleón-Cano et al. 2003). These semiarid climatic conditions inhibited formation of high concentrations of organic matter (mean = 0.77% $C_{organic}$; SD = 0.60; $n = 33$) and resulted in high pH (mean = 8.10; SD = 1.64; $n = 33$) in the soils of the district. However, the question here is whether these long lasting dry conditions were enough to compensate for the adverse mineralogical and structural setting of the district. Although metal and metalloid mobility-fixation in soils is thought to be related (among other factors) to the organic matter, pH, and binding oxide mineral phases (Kabata-Pendias 2001; Kumpiene et al. 2008; among others), none of the studied trace elements showed any statistically significant relationship to the first two. On the other hand, based on SEM-EDX studies, we found positive evidence for the binding of As and other metallic cations to Fe and Mn mineral oxide phases (Fig. 5a, b). Colloidal goethite (FeOOH) has a net positive charge in acid media (e.g., Seaman et al. 1997), which binds to the negatively charged arsenic complex ions by adsorption. These complex ions may remain strongly bound to goethite up to higher pH of 8.0–8.5 (Davis and Kent 1990; Smith 1999; Smedley and Kinniburgh 2002), as seems to be the case in some of the studied samples from the tailings (Fig. 5a). Desorption of arsenic from goethite may occur by competition between negative charges for the positive colloid, a reduction of the iron oxide mineral phase (Meng et al. 2002), or high pH values (>8.5). Given that redox conditions in the studied topsoil samples must be rather oxidative (as suggested by the very low contents of organic matter), reduction does not seem to be a plausible mechanism for As desorption. However, many of the pH values are above 8.5, which may provide an indication that As maintains some mobility in the superficial environment of the topsoils. If this is correct,

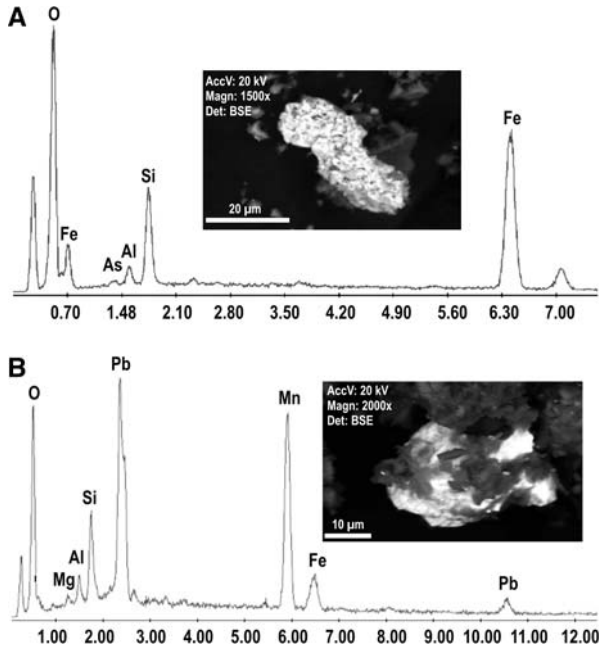

Fig. 5 EDX spectra and BSE images of mineral grains from samples: **a** RP-8: As bearing goethite-like grain, lower tailings; **b** RP-32: Pb-rich, coronadite-like grain, María Josefa mine

then the tailings and the heap leaching pile constitute potential sources for As migration. This is because the complex anions of this metalloid that cannot be adsorbed by goethite will migrate in solution either as $H_2AsO_4^-$ at pH = 2–7 (unlikely in the presently alkaline environment of Rodalquilar) or as $HAsO_4^{2-}$ at pH ≥ 7 (Smedley and Kinniburgh 2002). Besides, as shown by Ferrier (1999), there is ample evidence for strong mechanical dispersion of iron oxide mineral phases from the tailings down to El Playazo (Fig. 2a, b). Taking into account the ruinous state of the containing dams, this is the least to be expected. Although it goes beyond the scope of this work, we may further speculate about the ultimate fate of As contained in the tailings. There may be a case for two likely transport mechanisms of As to the coast: first, as arsenic bound to goethite (Fig. 5a), and second, as complex anions of the $HAsO_4^{2-}$ type. A similar conclusion, although at much lesser extent, can be drawn for Cu, Pb, and As, which have high concentrations in stream sediments up to 1 km downstream from the tailings (Wray 1998). On the other hand, the Mn oxide phases (Fig. 5b) may correspond to minerals of the type $A_{1-2}Mn_8O_{16}{\cdot}xH_2O$, where A can be Ba, K, Na or Pb (Roy 1981), such as the grains found in a topsoil from María Josefa (Fig. 2a, b). The accommodation of large cations such as Pb^{2+} in Mn oxides is not unusual [as in coronadite: $Pb(Mn^{4+},Mn^{2+})_8O_{16}$] but requires the presence of Mn^{2+} or Mn^{3+} in addition to Mn^{4+} in the linked [MnO_6] octahedra to maintain charge balance (Roy 1981). The structural fixation of metal cations such as Pb to Mn oxide phases of this type is therefore far more stable than in the case of the binding of As to goethite.

Metal and metalloids in the soils and plants

With the exception of Cd, trace element concentrations in the soils of the district are several orders of magnitude above local and world baselines (Table 3). Even if the results from the tailings are not considered, the concentrations are still very high compared to world averages (Table 3). In addition, two agricultural soils near to Cortijo del Fraile and the heap leaching pile yielded As concentrations of 159 (RP-38) and 104 µg g^{-1} (RP-40), well above our local baselines from Morrón de Mateo (MM baselines) and world averages (Fig. 1) (Tables 1, 3). A closer inspection of Table 3 reveals a conspicuous fact: some element concentrations increase in the tailings (As, Bi, Cu, Sb, Se, Te) whereas others have higher concentrations in the rest of the samples (Cd, Hg, Pb, Zn). Given that the tailings received the wastes from the cyanide metallurgical plant that treated the El Cinto ores (see sections on mineralogy of mineral deposits and metallurgy), the first group of elements can be regarded as derived from a common primary mineral assemblage. On the other hand, as shown above, Cd, Pb and Zn are the elements found in the ores from the peripheral deposits. Thus, the soils of the district reflect two well-differentiated metallogenic systems. In order to confirm or discard this assumption, we statistically studied the data population using cluster analysis, in order to analyze whether the elements grouped somehow reflecting the original chemistry of the mineral parageneses. The dendrograms show the existence of two main groups that match the metallic signature of the two types of ore deposits present in the district (Fig. 6a). As shown below, these relationships are not restricted to the soils but can also be observed in the studied plants species (Fig. 6b).

All plants accumulate metals at the trace element level; however, in some cases, metal accumulation may largely exceed these figures, with concentrations above 10,000 µg g^{-1} (e.g., Reeves et al. 1995). Plants having this potential are termed hyperaccumulators, and have been identified in at least 45 families and may reach metal concentrations of 10–1000 times higher than normal ones (Chaney et al. 1995; Cobbet 2003; among others). The interest on hyperaccumulators came first as biogeochemical tools for the exploration of mineral deposits (e.g., Kovalevski 1987; Reeves et al. 1995; among others), and later in phytoremediation for land reclamation in abandoned mining sites and districts (Chaney et al. 1995; Reeves et al. 1995; Cobbet 2003; among others). Besides, accumulation of metals by plants also serves as an indicator

Table 3 Mean concentrations for trace elements from Rodalquilar and the MM baselines

Element (μg g^{-1})	As	Bi	Cd	Cu	Hg	Pb	Sb	Se	Sn	Te	Zn	Reference
Rodalquilar												
All samples	461.3	8.4	0.4	92.5	0.44	366.1	20.5	16.5	26.9	4.5	216.0	This work
Tailings and pile	954.2	17.6	0.3	105.8	0.36	288.0	38.2	33.2	55.0	7.6	171.1	
Excluding tailings and pile	179.6	3.1	0.5	84.9	0.48	410.7	10.3	6.9	10.8	2.7	241.7	
Local baseline[a]												
Morrón de Mateo (MM) 1	21.0	<0.02	0.1	13.8	0.12	31.0	0.2	1.1	0.5	0.3	54.1	This work
Morrón de Mateo (MM) 2	5.3	<0.02	0.1	14.4	0.05	35.0	0.5	1.0	4.0	1.3	53.9	
Other sources												
Selected average for soils	5.8		0.06–1.1	13–24	0.03	32		0.33				Alloway (2005)
World soils			0.06	22		30					66	Callender (2004)
Various soils	7.2											Smedley and Kinniburgh (2002)
Averages and ranges	4.4–9.3	0.2	0.37–0.78	13–24	0.05–0.26	22–40	0.9	0.25–0.38	1.1	0.02–0.69[b]	45–100	Kabata-Pendias (2001)

[a] Volcanic soils (see Fig. 1 for location)

[b] US soils

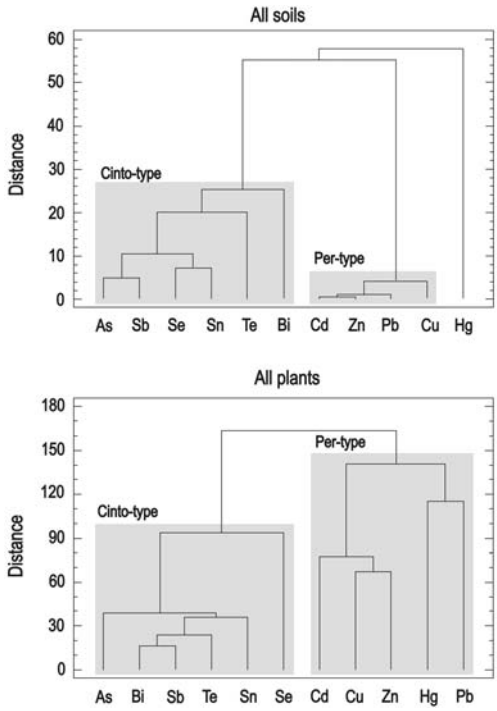

Fig. 6 Dendrogram (clusters by group average; distances: squared euclidean) for soils and plants showing the existence of two well-differentiated groups of elements. *On the left* chemical elements present in the El Cinto paragenesis. *On the right* chemical elements present in the peripheral (*Per*) deposits paragenesis

of environmental disturbances and potential health hazards for the human and animal life (e.g., Alloway 2005; Molina et al. 2006; among others).

All the studied plant species from Rodalquilar accumulate elements but only up to a certain level, and therefore cannot be regarded as hyperaccumulators (Table 2). Furthermore, compared to our local baselines (Morrón de Mateo: MM) for *A. horridus*, *L. arborescens*, *S. genistoides*, and *S. tenacissima*, only the concentrations of As, Bi, and Sb are clearly above the MM concentrations (Table 2). In this respect, a comprehensive study by McGrath and Zhao (2003) showed that despite the claims regarding the great potential of some plant species for decontaminating heavy metals from polluted soils, bioaccumulation factors (BF: element concentration in plant/element concentration in soil) are often below 0.2 for plants grown on contaminated soils. Conesa et al. (2007) reached a similar conclusion for *L. spartum* grown in mine tailings (with high contents of Cu, Zn, As, Cd, Pb) from SE Spain. These authors only found bioaccumulation factors above 0.2 for Cd and Zn, and suggested that low accumulation could be related to an exclusion strategy for metal tolerance. We found similar results for our plants species in the Rodalquilar district, with Cd, Hg and Zn being the only elements with a BF above 0.2 (Table 4). This is somehow reflected in poor correlations between the concentrations of element in soil—element in plant when single anomalous, high element concentration samples (outliers), are removed from the statistical analysis. One outlier can be enough to produce a high correlation coefficient even though the relationship between the two variables is nonexistent. On the other

Table 4 Bioaccumulation factors (BF: element concentration in plant/element concentration in soil) for the different plant species

	As	Bi	Cd	Cu	Hg	Pb	Sb	Se	Sn	Te	Zn
Asparagus horridus											
All samples											
Mean ($n = 14$)	0.0033	0.0960	0.2000	0.0440	0.0961	0.0042	0.0115	0.0825	0.0068	0.0073	0.4723
SD	0.0052	0.3465	0.2447	0.0359	0.1325	0.0058	0.0198	0.1007	0.0086	0.0182	0.3896
Tailings											
Mean ($n = 5$)	0.0020	0.0048	0.1518	0.0281	0.0647	0.0035	0.0086	0.0453	0.0038	0.0043	0.2089
SD	0.0012	0.0023	0.2241	0.0135	0.0358	0.0027	0.0039	0.0368	0.0015	0.0033	0.1123
Launaea arborescens											
All samples											
Mean ($n = 25$)	0.0049	0.1287	3.9859	0.2228	0.3114	0.0101	0.0119	0.2026	0.0080	0.0090	1.5236
SD	0.0083	0.6190	6.2083	0.2086	0.3582	0.0149	0.0168	0.3350	0.0135	0.0219	4.4412
Mean ($n = 10$)	0.0033	0.0039	1.7181	0.1475	0.1506	0.0036	0.0052	0.0985	0.0034	0.0047	0.2878
SD	0.0041	0.0071	2.3906	0.1501	0.1014	0.0039	0.0059	0.0835	0.0066	0.0093	0.2528
Lygeum spartum											
All samples											
Mean ($n = 14$)	0.0128	0.1853	0.9462	0.0547	0.1602	0.0173	0.0262	0.0796	0.0134	0.0163	1.6448
SD	0.0566	2.4000	2.7200	0.2027	0.0915	0.0915	0.1132	0.2652	0.0520	0.0755	17.5385
Mean ($n = 7$)	0.0087	0.0183	0.7930	0.0212	0.1630	0.0095	0.0234	0.1103	0.0128	0.0185	0.1672
SD	0.0110	0.0248	0.8201	0.0058	0.1052	0.0049	0.0197	0.0990	0.0176	0.0255	0.0769
Salsola genistoides											
All samples											
Mean ($n = 19$)	0.0051	0.1044	2.5120	0.1557	0.2204	0.0094	0.0108	0.0636	0.0075	0.0085	1.5768
SD	0.0073	0.4348	4.2551	0.1164	0.2712	0.0113	0.0091	0.0491	0.0109	0.0158	4.6884
Mean ($n = 7$)	0.0036	0.0051	2.4183	0.1019	0.1550	0.0096	0.0093	0.0541	0.0044	0.0068	0.5466
SD	0.0036	0.0046	4.5794	0.0541	0.0727	0.0069	0.0072	0.0459	0.0037	0.0068	0.4703
Stipa tenacissima											
All samples											
Mean ($n = 11$)	0.0047	0.1586	0.3356	0.0667	0.1774	0.0079	0.0087	0.0274	0.0071	0.0029	0.3573
SD	0.0081	0.5112	0.3739	0.0512	0.1522	0.0096	0.0061	0.0167	0.0064	0.0017	0.5613
Tailings (2 samples)											
RP9	0.0040	0.0083	1.1280	0.0923	0.2516	0.0177	0.0201	0.0169	0.0079	0.0045	0.1386
RP10	0.0029	0.0019	0.0818	0.0108	0.0328	0.0021	0.0044	0.0491	0.0014	0.0019	0.0532

hand, a simple inspection of data from soils and plants revealed that at least there was some correspondence between the concentrations of elements in soils and plants. Thus, we tried a different approach to the problem, this time based on canonical correlation analysis. The purpose of this analysis is to summarize the relationships between two sets of variables by finding a small number of linear combinations from each set of variables that have the highest correlation possible between the sets. A canonical correlation (Garson 2008) is the correlation of two canonical (latent) variables, one representing a set of independent variables, the other a set of dependent variables. Each set may be considered a latent variable based on measured indicator variables in its set. Elements considered here for the analysis are: As, Bi, Cd, Cu, Hg, Pb, Sb, Se, Sn, Te, Zn. In this case, the first set (independent variables) is formed by the concentrations of these elements in soils, whereas the second set (dependent variables) is formed by the concentrations of these elements in plants. We show the fitting to a linear model for the first two elements: As and Bi (Fig. 7). Satistical data for the canonical correlation are shown in Table 5. The good canonical correlation (CC = 0.85) and a P value of 0.00 at the 95% confidence level (Table 5) support a significant relationship (similar statistical behavior) between element concentration in soils and plants. At the intrapopulation level (elements in either plants or soils), higher correlations were found for As, Bi, Sb, Se, Sn, and Te (Fig. 8) (Table 6), whereas those for Pb, Zn, Cd, Hg, or Cu were much lower.

The case of mercury

Given that mercury was used in the late 1920s to amalgamate gold in Rodalquilar (María Josefa and Abellán mines) (Fig. 2b) we conducted a pilot survey for Hg (gas) in two sectors of the district. To obtain a baseline for Hg (gas) we measured continuously from San José to Las Amatistas (Fig. 1). For a total measuring time of 30 min (data acquisition every 10 s: 175 measurements) we obtained a mean value of 13.5 ng Hg m^3 (SD = 4.1). This figure is much higher than the baseline for the Mediterranean basin (in the order of 2–3 ng Hg m^{-3}) (Wängberg

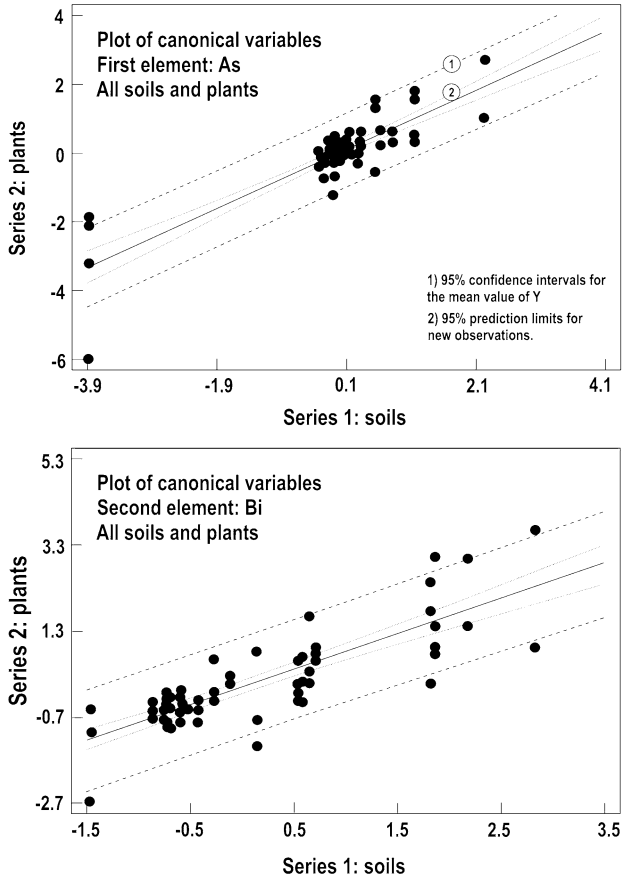

Fig. 7 Canonical correlation: fitting to a linear model for the first two elements: As and Bi. Independent variable (series 1): soils; dependent variable (series 2): plants. See also Table 5 for additional data on canonical correlation

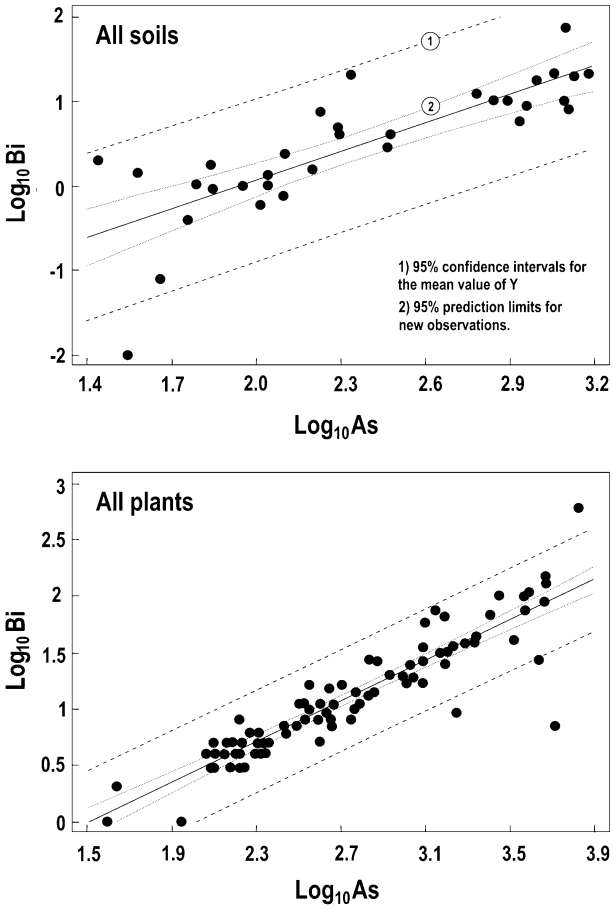

Fig. 8 Two examples of linear regression (log–log) at intrapopulation level: As and Bi in plants and soils. See also Table 6 for additional data

Table 5 Summary for canonical correlation analysis of elements in soils and elements in plants

Number	Eigenvalue	Canonical correlation	Wilks Lambda	Chi-Square	DF	*P* value
1	0.728921	0.853768	0.008470	336.368	121	0.0000
2	0.665625	0.815858	0.031247	244.341	100	0.0000
3	0.536188	0.732249	0.093449	167.109	81	0.0000
4	0.427178	0.653589	0.201481	112.945	64	0.0002
5	0.363753	0.603119	0.351734	73.6641	49	0.0129
6	0.206005	0.453878	0.552826	41.7862	36	0.2339
7	0.130898	0.361799	0.696258	25.5234	25	0.4334
8	0.128350	0.358260	0.801124	15.6326	16	0.4789
9	0.049810	0.223182	0.919090	5.94821	9	0.7451
10	0.028351	0.168377	0.967270	2.34610	4	0.6724
11	0.004507	0.067138	0.995493	0.318497	1	0.5725

DF degrees of freedom

Table 6 Correlation coefficients for *Cinto-type* element pairs (log–log) in soils (bold) and plants

Element	As	Bi	Sb	Se	Sn	Te
As		**0.81**	**0.88**	**0.86**	**0.95**	**0.67**
Bi	0.90		**0.71**	**0.69**	**0.84**	**0.40**
Sb	0.85	0.95		**0.81**	**0.86**	**0.74**
Se	0.49	0.43	0.39		**0.89**	**0.75**
Sn	0.70	0.81	0.82	0.31		**0.63**
Te	0.83	0.87	0.80	0.37	0.67	

et al. 2001) and may be merely reflecting the fact that hydrothermal phenomena in the Cabo de Gata volcanic block were widespread. For example, most of the older andesitic rocks display pervasive propylitic alteration. Data from the upper tailings and the María Josefa Mine are even higher. We obtained a mean value of 25.9 ng Hg m^3 (SD = 77.1) in the former ($n = 216$), and 43.6 ng Hg m^3 (SD = 96.7) in María Josefa ($n = 351$) where amalgamation was widely used in the past. On the other hand, given that the tailings correspond to the residues from cyanide ore treatment, we may infer that the higher Hg (gas) readings could be related to the presence of primary mercury (cinnabar) from the El Cinto ores. However, with the exception of one sample (RP-31: 1.4 μg g^{-1} Hg), we did not find high concentrations of this element in the tailings (Table 3). On the other hand, past amalgamation practices in the district may have influenced metal distribution. For example, samples RP-22 and 26 (close to Minas de Abellán) (Fig. 2b) have Hg concentrations of 2.6 and 0.8 μg g^{-1}, respectively, whereas at María Josefa sample RP-32 yielded a concentration 0.7 μg g^{-1} Hg. These may not be extremely high concentrations of mercury, but these soils are nevertheless highly enriched in this element compared to baselines, and in any case, these figures are above those from other sectors of the district (Table 1, 3).

Conclusions

This survey provides some useful insights into the environmental problems from past mining operations. This sensitive issue should be dealt with considering all the variables (natural and anthropic) involved in the process. For example, we must take into account that once erosion starts, the unroofing of a mineral deposit will inevitably lead to the sustained leaching of metals, and therefore, to long-lived natural contamination of the environment. In other words, mineral deposits are to be regarded as hot spots for long-lived metal contamination. However, whatever the degree and extent of the natural dispersion of metals and metalloids, the mining (anthropic) factor, involving from the relatively harmless road construction works to the truly damaging metallurgical operations, strongly aggravates the environmental risks. After more than a century of almost continuous mining and metallurgical activities for gold extraction, the Rodalquilar district can be presently regarded a severely polluted land site. As expected metal and metalloid dispersion in Rodalquilar have two intermingled sources: (1) the ore deposits themselves and mine operations; and (2) the metallurgical operations and derivative mineral wastes. Of all the studied elements arsenic appears as the most persistent pollutant in the district, with mean concentrations in tailings of 954 μg g^{-1}, whereas in the rest of samples this figures lowers to 180 μg g^{-1}, which is yet very high compared to those of the MM baselines (21.0 and 5.3 μg g^{-1}). Arsenic is bound to goethite in the tailings, but degradation and runoff has resulted in downstream iron oxide dispersion. The case in the heap leaching pile of El Cinto is no better and constitutes a matter of major concern. The huge pile is adjacent to presently active agricultural lands (Figs. 2a, b, 4b), and samples from the latter soils have 11–27 times more As than world averages, and 5–30 times the concentrations observed in the MM baselines (Tables 1, 3).

A definitive relationship between metals in soils and plants has been established. However, reduced absorption capabilities in the studied species may have prevented higher rates of bioaccumulation. This is important because the western side of the district is subjected to occasional shepherding of goats and lambs. However, although the studied plants do not have extremely high concentrations of metals and metalloids, they do accumulate As beyond the levels observed for the MM baselines (Table 2). For example, the plants have 2 (*L. arborescens*) to 8 (*S. tenacissima*) times the As concentrations found in the MM baselines. This enrichment goes further up if only the tailings are considered. In this case the plants have 4 (*L. arborescens*) to 30 (*S. tenacissima*) times the concentrations found in the MM baselines. Other cases of metal accumulation respect to the MM baselines are provided by *S. genistoides* (Cu and Zn) and *S. tenacissima* (Cu) (Table 2). Finally, beyond the hazards posed by metals and metalloids, other environmental concerns in Rodalquilar are worth to be at least briefly mentioned here: (1) the degradation state of the concrete dam containing the lower tailings (Fig. 4d); (2) the cavity forming processes in the upper tailings (Fig. 4e) involving removal of contaminated materials; (3) the existence of severely damaged buildings in the abandoned mining facilities (Fig. 4h) and unsealed galleries and shafts in the abandoned mines, which pose a safety risk for visitors; and (4) the transformation of old mining roads into actual rubbish dumps, which implies a serious degradation of the landscape (Fig. 4i).

Acknowledgments Valuable aid was received from ASM staff E.M. García Noguero (analyses of Hg in soils), M.A. López Berdonces (sample preparation), and J.M. Esbrí (technical support). We thank Francisco Carreño (URJC) for the DEM of the Rodalquilar district. This study was funded by the Spanish Ministry of Education (Project CTM2006-13091-C02-01) and the Castilla-La Mancha Regional Government (Project PCC-05-004-3). Both projects were cofunded by European Union FEDER grants.

References

Alloway BJ (2005) Bioavailability of elements in soil. In: Selinus O, Alloway B, Centeno JA, Finkelman RB, Fuge R, Lindh U, Smedley P (eds) Essentials of Medical Geology. Elsevier, Amsterdam, pp 347–372

Arribas A (1993) Mapa Geológico del Distrito de Rodalquilar (scale 1: 25, 000). Instituto Tecnológico Geominero de España, Madrid

Arribas A Jr, Cunningham CG, Rytuba JJ, Rye RO, Kelly WC, Podwysocki MH, McKee EH, Tosdal RM (1995) Geology, geochronology, fluid inclusions, and isotope geochemistry of the Rodalquilar gold alunite deposit, Spain. Econ Geol 90:795–822

Bhattacharyya KG, Gupta SS (2008) Adsorption of a few heavy metals on natural and modified kaolinite and montmorillonite: a review. Adv Colloid Interface Sci 140:114–131

Callender E (2004) Heavy metals in the environment—Historical trends. In: Lollar BS (ed) Treatise on geochemistry, vol 9. Elsevier, Amsterdam, pp 67–105

Chaney RL, Brown SL, Li YM, Angle JS, Homer FA, Green CE (1995) Potential use of metal hyperaccumulators. Min Environ Manag 3:9–11

Cobbet C (2003) Heavy metals and plants—model system and hyperaccumulators. New Phytol 159:289–293

Conesa HM, Robinson BH, Schulin R, Nowack B (2007) Growth of *Lygeum spartum* in acid mine tailings: response of plants developed from seedlings, rhizomes and at field conditions. Environ Pollut 145:700–707

Davis JA, Kent DB (1990) Surface complexation modeling in aqueous geochemistry. In: Hochella MF, White AF (eds) Mineral–water interface geochemistry. Reviews in Mineralogy, vol 23. Mineralogical Society of America, Washington DC, pp 177–260

De Baets S, Poesen J, Knapen A, Barberá GG, Navarro JA (2007) Root characteristics of representative Mediterranean plant species and their erosion-reducing potential during concentrated runoff. Plant Soil 294:169–183

Doblas M, Oyarzun R (1989) Neogene extensional collapse in the western Mediterranean (Betic-Rif Alpine orogenic belt): implications for the genesis of the Gibraltar Arc and magmatic activity. Geology 17:430–433

Ferrier G (1999) Application of imaging spectrometer data in identifying environmental pollution caused by mining at Rodaquilar, Spain. Remote Sens Environ 68:125–137

Garson D (2008) Canonical correlation: statnotes from North Carolina State University. Public Administration Program, http://www2.chass.ncsu.edu/garson/pa765/canonic.htm. Cited 24 April 2008

Heald P, Foley NK, Hayba D (1987) Comparative anatomy of volcanic-hosted epithermal deposits: acid sulfate and adularia-sericite types. Econ Geol 82:1–26

Hernández Ortiz F (2004) Rodalquilar: Historia Gráfica. GBG. Editora Ingoprint SA, Almería, p 118

Hernández F (2005) Rodalquilar, el oro del Cabo de Gata: Historia. Bocamina 15:18–30

Huibregtse P, Alebeek HV, Mattijs Z, Biermann C (1998) Palaeostress analysis of the northern Nijar and southern Vera basins: constraints for the Neogene displacement history of major strike-slip faults in the Betic Cordilleras, SE Spain. Tectonophysics 300:79–101

Kabata-Pendias A (2001) Trace elements in soils and plants. CRC Press, Boca Raton, p 413

Keller JVA, Hall SH, McClay KR (1997) Shear fracture pattern and microstructural evolution in transpressional fault zones from field and laboratory studies. J Struct Geol 19:1173–1187

Kovalevski AL (1987) Biogeochemical exploration for mineral deposits. VNU Science Press, Utrecht, p 224

Kumpiene J, Lagerkvista A, Mauricea C (2008) Stabilization of As, Cr, Cu, Pb and Zn in soil using amendments—a review. Waste Manag 28:215–225

McGrath SP, Zhao FJ (2003) Phytoextraction of metals and metalloids from contaminated soils. Curr Opin Biotechnol 14:277–282

Meng X, Korfiatis GP, Bang S, Bang KW (2002) Combined effects of anions on arsenic removal by iron hydroxides. Toxicol Lett 133:103–111

Molina JA, Oyarzun R, Esbrí JM, Higueras P (2006) Mercury accumulation in soils and plants in the Almadén mining district, Spain, one of the most contaminated sites on Earth. Environ Geochem Health 28:487–498

Montoya JW, Hemley JJ (1975) Activity relations and stabilities in alkali feldspar and mica alteration reactions. Econ Geol 70:577–583

Moreno T, Oldroyd A, McDonald I, Gibbons W (2007) Preferential fractionation of trace metals-metalloids into PM_{10} resuspended from contaminated gold mine tailings at Rodalquilar, Spain. Water Air Soil Pollut 179:93–105

Ormonde Mining (2002) Annual Report 2001. http://www.ormondemining.com/invest/finreports.html. Cited 24 April 2008

Ownby DR, Galvan KA, Lydy MJ (2005) Lead and zinc bioavailability to *Eisenia fetida* after phosphorus amendment to repository soils. Environ Pollut 136:315–321

Oyarzun R, Márquez A, Ortega L, Lunar R, Oyarzún J (1995) A late Miocene metallogenic province in southeast Spain: atypical Andean-type processes on a smaller scale. Trans Instn Min Metall Sect B: Appl Earth Sci 104:197–202

Oyarzun R, Lillo J, Higueras P, Oyarzún J, Maturana H (2004) Strong arsenic enrichment in sediments from the Elqui watershed, Northern Chile: industrial (gold mining at El Indio-Tambo district) vs. geologic process. J Geochem Explor 84:53–64

Oyarzun R, García Romero E, López García JA, Regueiro M, Molina JA (2007a) Teaching field geology in SE Spain: an alternative approach. European Geologist 24:9–12

Oyarzun R, Oyarzún J, Lillo J, Maturana H, Higueras P (2007b) Mineral deposits and Cu–Zn–As dispersion-contamination in stream sediments from the semiarid Coquimbo Region, Chile. Environ Geol 53:283–294

Pantaleón-Cano J, Yll EI, Pérez-Obiol R, Roure JM (2003) Palynological evidence for vegetational history in semi-arid areas of the western Mediterranean (Almería, Spain). The Holocene 13:109–119

Platt JP, Vissers RLM (1989) Extensional collapse of thickened continental lithosphere: a working hypothesis for the Alboran Sea and Gibraltar Arc. Geology 17:540–543

Plumlee GS (1999) The environmental geology of mineral deposits. In: Plumlee GS, Logsdon MJ (eds) The Environmental Geochemistry of Mineral Deposits (Part A: Processes, Techniques, and Health Issues, Reviews in Economic Geology 6A:71–116. Society of Economic Geologists, Littleton

Plumlee GS, Smith KS, Montour MR, Ficklin WH, Mosier EL (1999) Geological controls on the composition of natural waters and mine waters draining diverse mineral-deposits types. In: Plumlee GS, Logsdon MJ (eds) The Environmental geochemistry of mineral deposits (Part B: Case studies and research topics),

Reviews in Economic Geology. Society of Economic Geologists, Littleton 6B:373–432
Reeves RD, Baker AJM, Brooks RR (1995) Abnormal accumulation of trace metals by plants. Min Environ Manag 3:4–8
Rossiter DG (2005) Proposal for a new reference group for the World Reference Base for Soil Resources (WRB): the Technosols. http://www.itc.nl/~rossiter/research/suitma/UrbWRB2006v2.pdf. Cited 24 April 2008
Roy S (1981) Manganese deposits. Academic Press, London, p 485
Rytuba JJ, Arribas A Jr, Cunningham CG, McKee EH, Podwysocki MH, Smith JG, Kelly WC, Arribas A (1990) Mineralized and unmineralized calderas in Spain; Part II, evolution of the Rodalquilar caldera complex and associated gold-alunite deposits. Mineral Deposita 25:S29–S35
Sagredo R (1987) Flora de Almería. Plantas Vasculares de la Provincia. Instituto de Estudios Almerienses, Almería, p 552
Seaman JC, Bertsch PM, Strom RN (1997) Characterization of colloids mobilized from southeastern coastal plains sediments. Environ Sci Technol 31:2782–2790
Sholupov SE, Ganeyev AA (1995) Zeeman absorption spectrometry using high frequency modulated light polarization. Spectrochim Acta 50B:1227–1238
Smedley PL, Kinniburgh DG (2002) A review of the source, behaviour and distribution of arsenic in natural waters. Appl Geochem 17:517–568
Smith KS (1999) Metal sorption on mineral surfaces: an overview with examples relating to mineral deposits. In: Plumlee GS, Logsdon MJ (eds) The environmental geochemistry of mineral deposits. Reviews in Economic Geology 6A:161–182, Society of Economic Geologists, Chelsea
Spaargaren O, Nachtergaele F (1998) Topsoil characterization for sustainable land management. Food and Agriculture Organization of the United Nations, Rome. ftp://ftp.fao.org/agl/agll/docs/topsoil.pdf. Cited 24 April 2008
Van Reeuwijk LP (2002) Procedures for soil analysis. Technical Paper 9, ISRIC, Wageningen, http://www.isric.org/Isric/Webdocs/Docs/ISRIC_TechPap09_2002.pdf. Cited 24 April 2008
Wängberg I, Munthe J, Pirrone N, Iverfeldt A, Bahlman E, Costa P, Ebinghaus R, Feng X, Ferrara R, Gardfeldt K, Kock H, Lanzillotta E, Mamane Y, Mas F, Melamed E, Osnat Y, Prestbo E, Sommar J, Schmolke S, Spain G, Sprovieri F, Tuncel G (2001) Atmospheric mercury distribution in northern Europe and in the Mediterranean region. Atmos Environ 35:3019–3025
Wray DS (1998) The impact of unconfined mine tailings and anthropogenic pollution on a semi-arid environment—an initial study of the Rodalquilar mining district, south east Spain. Environ Geochem Health 20:29–38